



Ultrasound-assisted homogeneous photocatalytic degradation of Reactive Blue 4 in aqueous solution

J.M. Monteagudo*, A. Durán, I. San Martín, S. García

University of Castilla-La Mancha, Grupo IMAES, Department of Chemical Engineering Escuela Técnica Superior de Ingenieros Industriales—INEI, Avda, Camilo José Cela, 1, 13071 Ciudad Real, Spain

ARTICLE INFO

Article history:

Received 27 November 2013

Received in revised form 5 January 2014

Accepted 9 January 2014

Available online 20 January 2014

Keywords:

RB4

Wastewater

Photo-Fenton

Sonolysis

ABSTRACT

The catalytic degradation of Reactive Blue 4 (RB4) by an emerging ultrasound-assisted photo-Fenton process with artificial ultraviolet light was investigated. The photocatalytic degradation efficiency was determined by the decrease in Total Organic Carbon (TOC) content. The influences of pH and initial concentrations of Fe(II) and H₂O₂ on the RB4 solution mineralization were studied. Under the optimal conditions, TOC removal increased up to 94% in 60 min, and this system permitted the use of a low ferrous concentration of only 5 mg L⁻¹. The RB4-mineralization process in the sono-photo-Fenton system can be described by a mechanism involving mineralization by direct photolysis, ultrasonically generated oxidative species, direct oxidation reaction with H₂O₂, radical reaction (mainly HO[•]) and thermal pyrolysis inside the bubble. The radical reaction in the bulk solution or in the vicinity of the bubble was found to be the main mineralization pathway. The contribution of different mechanisms to overall mineralization was the following: radical reaction (93.60%), direct reaction with H₂O₂ (2.56%), photolysis (1.92%) and reaction by ultrasonically generated oxidative species (1.92%). The influence of the Fe catalyst on the radical reaction was evaluated by conducting the reaction in the presence and absence of the scavenging agent potassium iodide (KI). The toxicity profile of sono-photo-Fenton process was also evaluated.

© 2014 Elsevier B.V. All rights reserved.

1. Introduction

Reactive dyes are extensively used in the textile industry. Under typical reactive dyeing conditions, up to 50% of the initial dye remains in the spent dyebath in its hydrolyzed form resulting in effluent containing high levels of organic and color contaminants [1]. The color and toxicity of dyes influence the quality of life by causing health problems, in addition to influencing the efficiency of some water treatment techniques. One of the major difficulties in treating this type of colored wastewater is that biological processes tend to be ineffective despite the fact that they are generally more economic in comparison with other treatments options [2,3]. Conventional treatment processes for textile wastewater usually involve coagulation–flocculation, adsorption, and activated sludge, all of which are quite ineffective for the decoloration of wastewater due to the high molecular weight and high water solubility. Additionally, these processes do not destroy or degrade dyes; they only remove them physically from the effluent, leaving sludge for eventual disposal in landfills [4–6].

In order to overcome these weaknesses, efficient treatments of these effluents by the so-called advanced oxidation processes (AOPs) such as ozonation, photocatalysis, Fenton or a combination of photo-Fenton, UV/O₃, UV/H₂O₂, UV/TiO₂ have been developed in the last decades [7–9]. In addition, ultrasonic dye degradation in the homogeneous and heterogeneous solutions as basic or auxiliary process for dye remediation has also been widely studied [10]. These studies have shown that ultrasonic irradiation alone is ineffective for dye degradation, but quite effective when combined with other AOPs [11–15]. The sonochemical reaction pathways for the degradation of pollutants species involve the reaction with hydroxyl radicals and a thermal reaction. The hydroxyl radicals are produced by the sonolysis of water as the solvent inside the collapsing cavitation bubbles under extremely high temperature and pressure [16]. The ultrasound-induced splitting of water molecules causes the reactions shown in Eqs. (1)–(6) [17–19].



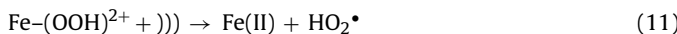
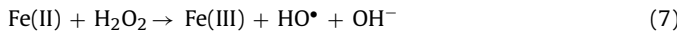
* Corresponding author. Tel.: +34 926295300x3888; fax: +34 926295361.

E-mail address: josemaria.monteagudo@uclm.es (J.M. Monteagudo).





The hydroxyl radicals generated by sonolysis can react with the dye molecule and a large majority of them are recombined to H_2O_2 inside the cavitation bubble and at the gas–liquid interface before being ejected into the bulk solution. Depending on the frequency of irradiation and applied power, only a small fraction of HO^\bullet escape from the interfacial region and diffuse into the bulk solution [20]. Alternatively, compounds inside or in the vicinity of a collapsing bubble may undergo pyrolytic decomposition due to the high local temperature and pressure [21]. It is generally believed that hydrophilic and non-volatile compounds mainly degrade through hydroxyl radical mediated reactions in the bulk solution, while hydrophobic and volatile species degrade thermally inside or in the vicinity of the bubble [22]. Previous studies have demonstrated that the addition of chemicals, such iron ions or combination with UV radiation, can amplify ultrasonic action [23,24]. Among these combination methods, photo-Fenton system in conjunction with ultrasonic irradiation (sono-photo-Fenton) produces extra hydroxyl radicals, regenerates Fe(II) and promotes the rate of degradation of pollutants [25–27] according to the following reactions:



Anthraquinone dyes constitute the second largest class of textile dyes after azo dyes, and they are used extensively in the textile industry. Reactive Blue 4 (RB4) was selected as model reactive anthraquinone dye for this investigation. Recently, many AOPs using Fenton reaction with or without UV light, heterogeneous catalysts such as TiO_2 combined with artificial UV or solar light sources or solar photocatalytic-Fenton system have been evaluated for the decoloration and degradation of RB4 dye. Neppolian et. al. reported that direct solar light induced and TiO_2 process achieved complete degradation of 4×10^{-4} M RB4 solution within 8 h in the presence of 300 mg L⁻¹ of H_2O_2 [28]. Photo-Fenton degradation of RB4 was investigated and 75% TOC removal of 20 mg L⁻¹ RB4 solution after nearly 120 min at pH 2 in the presence of 300 mg L⁻¹ of H_2O_2 and 4 mg L⁻¹ of Fe^{2+} was attained [29]. Photo-Fenton process under artificial and solar irradiation of RB4 was studied and the best results were obtained using 1.0 mM ferrioxalate and 10 mM of H_2O_2 . In this case, 80% TOC and 100% of color removal were obtained for 0.1 mM RB4 dye in 35 min of solar irradiation [30]. The heterogeneous photocatalytic mineralization of RB4 solution under a UV/Fenton/ TiO_2 system with concentrated solar light irradiation using a Fresnel lens was also studied. After 120 min, total decoloration was reached, whereas only 50% of TOC was removed [31]. The effect of operational conditions on decoloration of RB4 solutions using zero-valent iron reductive transformation has been reported [32]. 90% color removal of RB4 solution was achieved by combined $\text{Fe(III)}/\text{TiO}_2$ catalyst and ultrasonic irradiation but no data of mineralization were presented [15]. To our knowledge, no study of mineralization of RB4 solution under homogeneous sono-photo-Fenton process has also been reported to date.

The aim of our work was to study the decoloration and mineralization of RB4 solutions by low frequency (24 kHz) ultrasonic irradiation in conjunction with photo-Fenton's reagent (sono-photo-Fenton system). An initial comparative study on RB4 mineralization by using different degradation systems has been carried out. The effects of pH and initial concentrations of Fe(II) and H_2O_2 on mineralization reaction by the sono-photo-Fenton process were determined. Finally, a kinetic and degradation mechanism study of the sono-photo-Fenton process was performed. The toxicity profile of such treatment was evaluated.

2. Experiment

2.1. Materials

RB4 ($\text{C}_{23}\text{H}_{14}\text{Cl}_2\text{N}_6\text{O}_8\text{S}_2$) solutions were prepared from pure compound purchased from Aldrich. $\text{FeSO}_4 \cdot 7\text{H}_2\text{O}$ (Panreac, analytical grade) and hydrogen peroxide (30% w/v, Merck) were used as received. pH was previously adjusted (between 2 and 8) by using 0.1 M H_2SO_4 and 6 M NaOH solutions. The initial concentration of TOC in the RB4 solution was always 30 mg L⁻¹.

2.2. Experimental runs

All experiments were carried out in a 400-mL stirred photoreactor with an external jacket connected to a thermostatic bath to maintain a constant temperature ($30 \pm 0.5^\circ\text{C}$). A Heraeus UV Hg immersed lamp TNN 15/32 with a nominal output of 15 W and emitting a monochromatic radiation at 254 nm was used to irradiate the solution. The UV-radiation intensity of the UV-lamp as measured with potassium ferrioxalate was 7.81×10^{-6} Einsteins s⁻¹. A 24 kHz, 200 W direct immersion horn sonicator (UP200S with an S14 sonotrode, Hielscher) was used to generate ultrasonic sound waves in the sonoreactor. The amplitude of the oscillatory system (power output) can be steplessly adjusted between 20% and 100%. The pulse mode factor (cycles) can be continuously varied between 10% and 100%. The set value equals the acoustic irradiation time in seconds, the difference to 1 s is the pause time. Thus, a setting of 1 implies that it is continuously switched on, whereas a setting of 0.6 means a power discharge of 0.6 s and a pause of 0.4 s. Amplitude and pulse length (cycles) were maintained constant at 60% and 1%, respectively.

The scavenging of hydroxyl radicals was accomplished with potassium iodide to quantify the oxidation levels from radical reactions. Before data analysis was done, all samples were withdrawn from the reactor for H_2O_2 analysis and immediately treated with excess Na_2SO_3 solution to prevent further oxidation (this procedure was performed to prevent an overestimation of the degradation).

2.3. Analysis

The mineralization grade of RB4 solution was determined by TOC variation, which was measured with a TOC-5050 Shimadzu analyzer (standard deviation < 0.2 mg L⁻¹). The H_2O_2 content in the solution was determined by titration through an aqueous solution of potassium permanganate (0.02 M) using an automatic Titrino SET/MET 702 (Metrohm). The ferrous concentration was obtained via photometric measurement with 1,10-phenanthroline (according to ISO 6332) using a UV–Vis spectrophotometer (Zuzi 4418PC). Toxicity was evaluated by determining the inhibitory effect of water samples on the light emission of *Vibrio fischeri* (Luminescent bacteria test; 30 min incubation time) using a

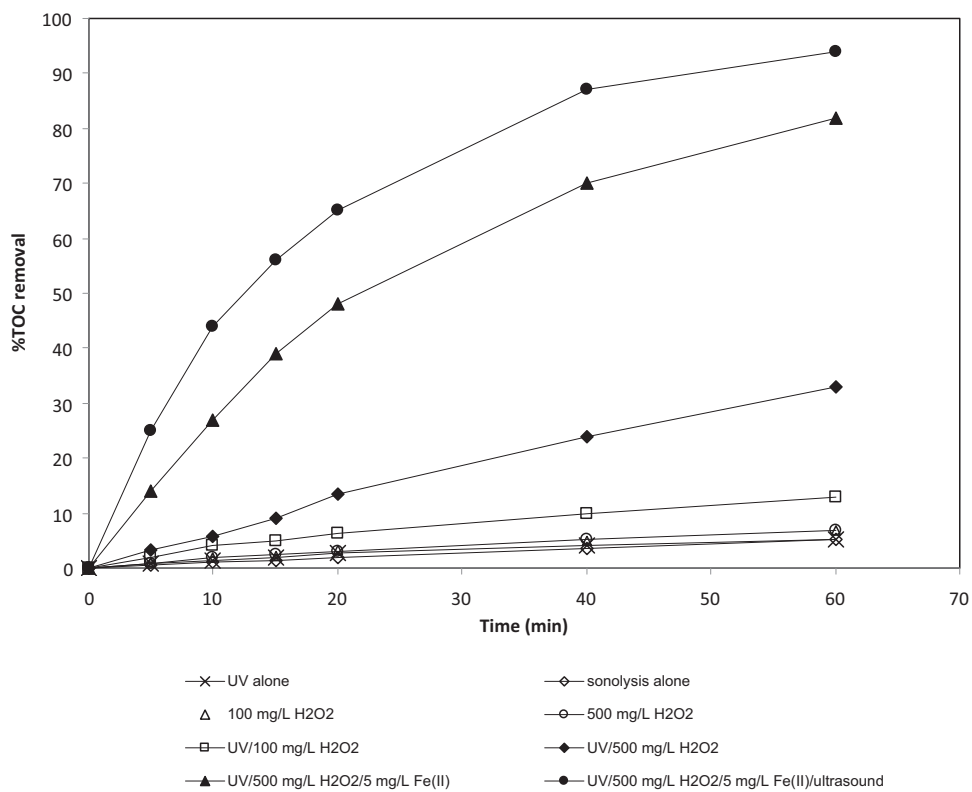


Fig. 1. Mineralization of RB4 solution under different reaction systems. $[\text{TOC}]_0 = 30 \text{ mg L}^{-1}$; $\text{pH} = 3$. Reaction time = 60 min. UV lamp (15 W, 254 nm); amplitude = 60%; pulse length (cycles) = 1.

luminometer (Optocomp BG-1, Gomensoro) according to ISO 11,348-3:1998.

3. Results and discussion

3.1. Comparative study

Fig. 1 shows the results of an initial comparative study on the mineralization of a RB4 solution ($[\text{TOC}]_0 = 30 \text{ mg L}^{-1}$) at pH 3 under different degradation systems. Reaction time was 60 min in all experiments. As can be seen, mineralization of RB4 solution via direct photolysis (UV alone) using an artificial UV-C light was very inefficient (%TOC removal = 5%). The results also confirmed the negligible effect of H_2O_2 as a single oxidant (%TOC removal = 6.8 or 7.0% using 100 or 500 mg L⁻¹ H_2O_2 , respectively) which indicated that direct or molecular reaction between peroxide and RB4 molecules was insignificant. The use of UV-C light in the presence of only Fe(II) did not improve the RB4 degradation (%TOC removal = 5%, data not shown) due to the fact that oxidative intermediate species (mainly hydroxyl radicals) are not generated under UV-C light irradiation of ferrous ions in the absence of H_2O_2 . When the RB4 solution was irradiated with UV-C light in the presence of 100 mg L⁻¹ or 500 mg L⁻¹ H_2O_2 , the degree of mineralization was increased to 13% or 33%, respectively. In these cases, as is well-known, hydroxyl radicals were generated by 254 nm photolysis of hydrogen peroxide, which indicates the favorable synergistic effect of H_2O_2 and UV-C light. Although HO^\bullet radicals are produced in this (UV/ H_2O_2) system, their concentration was not sufficient to achieve a high degree of mineralization of RB4 solution. The treatment with UV-C assisted Fenton reagent (photo-Fenton system; UV/5 mg L⁻¹ Fe(II)/500 mg L⁻¹ H_2O_2) led to 82% TOC removal in 60 min. The increased degradation efficiency could be due to the continuous regeneration of Fe(II) via photoreduction of Fe(III) (Eq.

(9)) and extra generation of hydroxyl radicals by this reaction and by Fenton reaction (Eq. (7)) [33].

Ferric ions were formed by the oxidation of ferrous ion (added as FeSO_4) by dissolved oxygen (Eq. (15)), by Fenton reaction (Eq. (7)) and by reaction (12).



As it is shown in **Fig. 1**, when the RB4 solution was treated by ultrasonic irradiation alone, the degree of mineralization was merely about 5% within 60 min of reaction. Although hydroxyl radicals can be produced by the sonolysis of water as indicated above (Eqs. (1)–(6)), they are most likely not produced in sufficient quantities to achieve a high degree of mineralization.

In order to increase the degree of mineralization, 5 mg L⁻¹ Fe(II) and 500 mg L⁻¹ H_2O_2 were introduced into RB4 solution before sonication and UV-C light irradiation. In this case, the mineralization of RB4 solution was conducted using the photo-Fenton process in conjunction with ultrasonic irradiation (sono-photo-Fenton process). 94% TOC removal was achieved within 60 min of reaction due to the enhancement in the production of HO^\bullet radicals. In sono-photo-Fenton reaction (as indicated above), HO^\bullet radicals are generated in two reactions. The ultrasonic wave can induce the dissociation of H_2O into HO^\bullet and H^\bullet , and H^\bullet can induce the dissociation of H_2O_2 into HO^\bullet and H_2O . Besides, Fe(II) is formed by reaction between H^\bullet and Fe(III) (Eq. (13)). Each Fe(II) ion can produce HO^\bullet and Fe(III) by Fenton reagent. Ferric ions on exposure to light decomposes water into a proton and HO^\bullet radical and Fe(III) is reduced to Fe(II) (Eq. (9)). The process is a cyclic one. Extra generation of hydroxyl radicals enhances the degree of mineralization. The participation of hydroxyl radicals as an active oxidizing species was confirmed by using a hydroxyl radical scavenger like potassium iodide (KI), where the rate of degradation was drastically reduced, as indicated below.

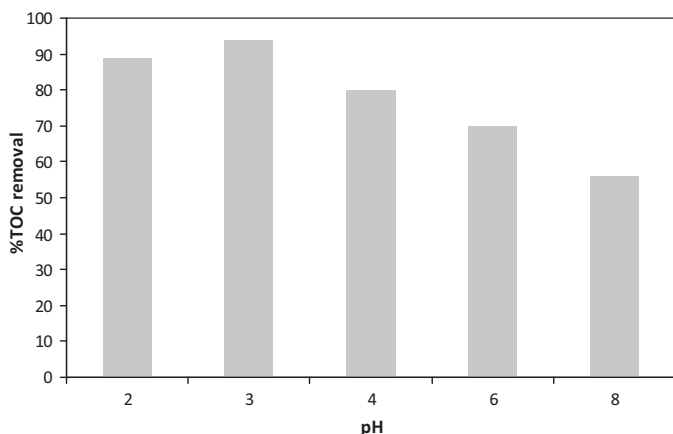


Fig. 2. Effect of pH on mineralization efficiency by using sono-photo-Fenton treatment. $[\text{TOC}]_0 = 30 \text{ mg L}^{-1}$; $[\text{Fe(II)}]_0 = 5 \text{ mg L}^{-1}$; $[\text{H}_2\text{O}_2]_0 = 500 \text{ mg L}^{-1}$; UV lamp (15 W, 254 nm); amplitude = 60%; pulse length (cycles) = 1; reaction time = 60 min.

3.2. Sono-photo-Fenton process

3.2.1. Effect of pH

Mineralization of RB4 solution ($[\text{TOC}]_0 = 30 \text{ mg L}^{-1}$; $[\text{Fe(II)}]_0 = 5 \text{ mg L}^{-1}$; $[\text{H}_2\text{O}_2]_0 = 500 \text{ mg L}^{-1}$; UV lamp (15 W, 254 nm); amplitude = 60%; pulse length (cycles) = 1; reaction time = 60 min) was carried out at different pH levels (2–8) under the sono-photo-Fenton process. Fig. 2 shows the effect of pH on mineralization efficiency. As can be seen, mineralization was improved at acidic conditions. On the one hand, it is well known that the optimum pH for photo-Fenton reaction is about 3. On the other hand, protonation of negatively charged $-\text{SO}_3^-$ groups in acidic medium occurs. The hydrophobic character enrichment of the resulting dye molecule enhances its reactivity under ultrasound treatment. Acidic conditions enhance the probability of the RB4 dye approaching to the negatively charged cavity bubbles where HO^\bullet radicals generated by sonolysis are most abundant [5]. However, at low pH values below 3, efficiency of TOC removal decreased due to HO^\bullet radical could be consumed by the scavenging effect of H^+ , and H_2O_2 could capture a proton to form hydroperoxonium ion (H_3O_2^+) that would cause hydrogen peroxide to become electrophilic, enhance its stability, and reduce reactivity between hydrogen peroxide and ferrous ions [34]. Moreover, the mineralization was inhibited when pH increased above 3 due to partial dye hydrolysis. The dye loses hydrogen atoms (from the protonated sites $-\text{SO}_3\text{H} \rightarrow -\text{SO}_3^-$) and both chloride atoms and gains hydroxyl groups, making it more hydrophilic. Under extreme alkaline conditions, HO^\bullet scavenging effects in the presence of anions such as HCO_3^- and CO_3^{2-} become more significant, and RB4 solution mineralization rate decreases. In addition, at the high pH values, Fe(III) precipitates in the form of hydroxide, and the oxidation potential of HO^\bullet also decreases, thus the RB4 mineralization rate also decreases.

3.2.2. Effect of Fe(II)

Mineralization of RB4 solution ($[\text{TOC}]_0 = 30 \text{ mg L}^{-1}$; pH = 3; $[\text{H}_2\text{O}_2]_0 = 500 \text{ mg L}^{-1}$; UV lamp (15 W, 254 nm); amplitude = 60%; pulse length (cycles) = 1; reaction time = 60 min) was carried out by the sono-photo-Fenton process at different initial concentrations of Fe(II), in the range $2.5\text{--}6 \text{ mg L}^{-1}$. The results are shown in Fig. 3. It was found that the TOC removal increased when the initial Fe(II) concentration increased from 2.5 mg L^{-1} to 5 mg L^{-1} . The ultrasonically generated H_2O_2 and the H_2O_2 added to the solution react with Fe(II) according to the Fenton reaction (Eq. (7)) to produce HO^\bullet radicals and so the Fe(II) can increase the degree of mineralization of RB4 solution via Eqs. (7), (10) and (11). The $\text{Fe}-\text{OOH}^{2+}$ formed

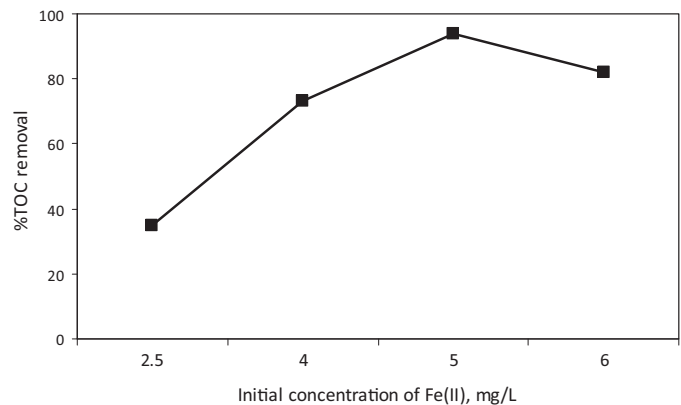
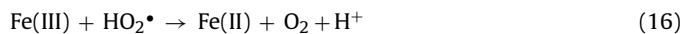


Fig. 3. Effect of the initial concentration of Fe(II) on the mineralization of RB4 solution by sono-photo-Fenton process. $[\text{TOC}]_0 = 30 \text{ mg L}^{-1}$; pH = 3; $[\text{H}_2\text{O}_2]_0 = 500 \text{ mg L}^{-1}$; UV lamp (15 W, 254 nm); amplitude = 60%; pulse length (cycles) = 1; reaction time = 60 min.

in these reactions can be decomposed into Fe(II) and hydroperoxyl radical (HO_2^\bullet) by ultrasonic irradiation (Eq. (11)) [35]. Fe(II) is formed again by reaction between Fe(III) and hydroperoxyl radical according to Eq. (16).



The re-formed Fe(II) could then react with H_2O_2 again as per the above equations and a closed cycle catalytic mechanism is then established. The increase in mineralization of RB4 solution is due to Fe(II) playing the role of a catalyst and initiating the decomposition of H_2O_2 to generate the hydroxyl radicals. The results also indicate that there is an optimum Fe(II) concentration (5 mg L^{-1}) for mineralization of RB4 solution by sono-photo-Fenton process with maximal efficiency. An excessive amount of Fe(II) leads to a decrease in the mineralization degree due to the scavenging of hydroxyl radicals by Fe(II) ions as in Eq. (12).

3.2.3. Effect of H_2O_2

The effect of the initial concentration of H_2O_2 on the sono-photo-Fenton reaction was studied using 5 mg L^{-1} Fe(II) and different hydrogen peroxide concentrations, in the range $100\text{--}600 \text{ mg L}^{-1}$ ($[\text{TOC}]_0 = 30 \text{ mg L}^{-1}$; pH = 3; UV lamp (15 W, 254 nm); amplitude = 60%; Pulse length (cycles) = 1). Fig. 4 shows the TOC removal of RB4 solution over a reaction time of 60 min. It can be seen that with the addition of 100, 300 and 500 mg L^{-1} hydrogen peroxide for the same amount of Fe(II) (5 mg L^{-1}) %TOC

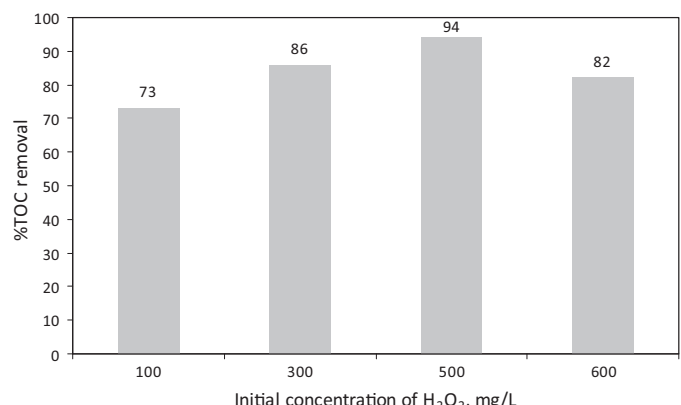


Fig. 4. Effect of the initial concentration of H_2O_2 on the mineralization of RB4 solution by sono-photo-Fenton process. $[\text{TOC}]_0 = 30 \text{ mg L}^{-1}$; pH = 3; $[\text{Fe(II)}]_0 = 5 \text{ mg L}^{-1}$; UV lamp (15 W, 254 nm); amplitude = 60%; pulse length (cycles) = 1; reaction time = 60 min.

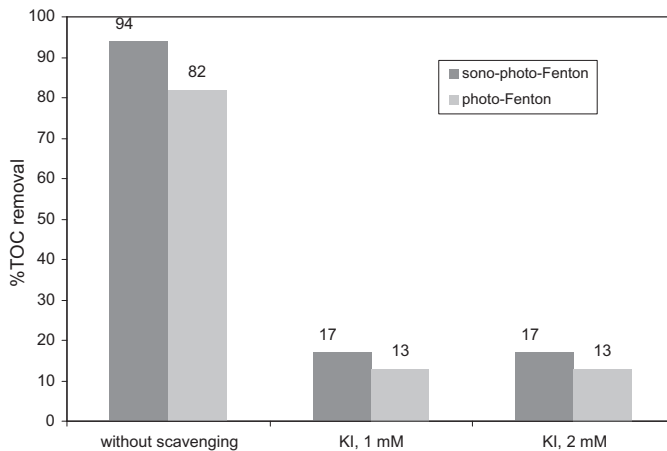


Fig. 5. Role of hydroxyl radicals in the mineralization of RB4 solution by the sono-photo-Fenton or photo-Fenton processes in the presence of 1 or 2 mM scavenging agent potassium iodide, KI. Operating conditions: $[TOC]_0 = 30 \text{ mg L}^{-1}$; pH: 3; $[H_2O_2]_0: 500 \text{ mg L}^{-1}$; $[Fe(II)]_0 = 5 \text{ mg L}^{-1}$; UV lamp (15 W, 254 nm); amplitude = 60%; pulse length (cycles) = 1; reaction time = 60 min.

removal increased from 73% to 86% and 94%, respectively. More hydroxyl radicals are generated with the presence of H_2O_2 in the irradiating solution due to the decomposition of H_2O_2 by photolysis and by Fenton reaction. However, when the hydrogen peroxide concentration was increased further (from 500 to 600 mg L^{-1}) the degree of mineralization decreased due to the scavenging effect of H_2O_2 towards HO^\bullet radicals when it is present in higher concentration. This reaction produces HO_2^\bullet radicals which are less reactive than HO^\bullet radicals. The produced HO_2^\bullet radical reacts rapidly with the hydroxyl radical according to Eq. (8). This suggests that the most appropriate initial concentration of H_2O_2 for the sono-photo-Fenton reaction was 500 mg L^{-1} under the operating conditions used in this study.

3.2.4. Radical reaction analysis

To quantify the oxidation levels by free radical reactions, the scavenging of HO^\bullet was accomplished with potassium iodide (HO^\bullet quencher) [36]. Several experiments were carried out using the sono-photo-Fenton process under the optimal operating conditions ($[Fe(II)]_0 = 5 \text{ mg L}^{-1}$; $[H_2O_2]_0 = 500 \text{ mg L}^{-1}$; pH = 3; $[TOC]_0 = 30 \text{ mg L}^{-1}$; UV lamp (15 W, 254 nm); Amplitude = 60%; Pulse length (cycles) = 1) in the presence or absence of KI. The role of hydroxyl radicals is shown in Fig. 5. As can be seen, the presence of 1 or 2 mM KI inhibited the mineralization reaction (the %TOC removal decreased as compared with the scavenger free reaction from 94% to 17%). This indicates the participation of hydroxyl radical in the reaction. Hydroxyl radicals were found to be the primary species contributing to the mineralization of RB4 solution by the sono-photo-Fenton process. Pyrolytic reaction and the RB4 diffusion inside the hot cavitation bubble are negligible. Pyrolytic reaction inside the cavitation bubbles may be excluded since mineralization would occur without interference from KI. In the presence of KI (hydroxyl radical scavenger), mineralization was practically negligible. RB4 dye is not volatile enough (low vapor pressure) to reach the bubble interior. On the other hand, at acid pH, the hydrophobic character enrichment of the resulting RB4 molecule enhances its reactivity in the vicinity of the bubble. It can be concluded that RB4 molecule gets degraded primarily at the bulk liquid or the bubble–liquid interface by hydroxyl radicals.

The mineralization of RB4 solution under photo-Fenton reaction (see Fig. 5) was also studied in the presence or absence of KI in the same conditions ($[Fe(II)]_0 = 5 \text{ mg L}^{-1}$; $[H_2O_2]_0 = 500 \text{ mg L}^{-1}$; pH = 3; $[TOC]_0 = 30 \text{ mg L}^{-1}$; UV lamp (15 W, 254 nm)). The presence

of KI also inhibited the mineralization reaction (the %TOC removal decreased from 82% to 13%). The difference between the degree of mineralization achieved with sono-photo-Fenton (17%) and photo-Fenton (13%) reactions in the presence of KI was due to the formation of small amounts of oxidative species by ultrasonic irradiation (H^\bullet , HO_2^\bullet , H_2O_2). These species were not quenched by KI and play a minimal role in mineralization.

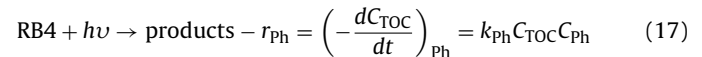
3.2.5. Kinetic and degradation mechanism study

As can be seen in Fig. 6, all the studied degradation systems (UV alone, sonolysis alone, single H_2O_2 , UV/ H_2O_2 , photo-Fenton and sono-photo-Fenton) fitted the pseudo-first order kinetics. Mineralization results obtained in these experiments were used to evaluate the possible degradation mechanisms.

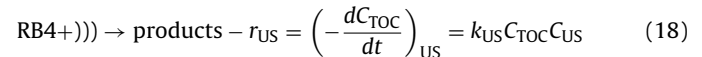
The results shown in Table 1 revealed that the RB4 mineralization by the sono-photo-Fenton system can be described by a mechanism involving mineralization by direct photolysis, ultrasonic irradiation (by ultrasonically generated oxidative species such as H^\bullet , HO_2^\bullet , H_2O_2 or HO^\bullet), direct oxidation reaction with H_2O_2 , radical reaction (mainly with HO^\bullet) and thermal pyrolysis inside the bubble.

The objective of this section was to determine the contribution of each of these mechanisms to the overall mineralization reaction. Thus, it was assumed that the reaction mechanism for the RB4 mineralization was split into five individual steps:

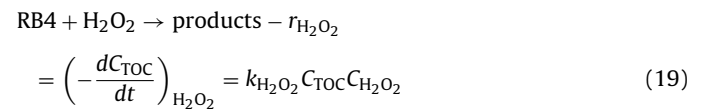
(1) Direct photolysis:



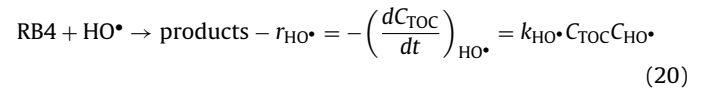
(2) Reaction by ultrasonically generated oxidative species:



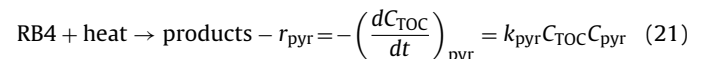
(3) Direct or molecular reaction with H_2O_2 :



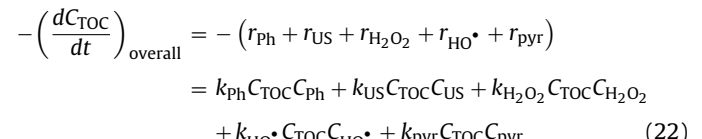
(4) Oxidation by free radicals (mainly HO^\bullet):



(5) Pyrolytic decomposition



Then, the overall rate of RB4 mineralization can be expressed as a sum of the contributions of Eqs. (17)–(21) as follows:



where r_{Ph} , r_{US} , $r_{H_2O_2}$, r_{HO^\bullet} and r_{pyr} represent the photolytic breakdown, degradation by ultrasonically generated oxidative species, molecular/direct reaction with H_2O_2 , radical reaction and thermal decomposition rates, respectively. k_{Ph} , k_{US} , $k_{H_2O_2}$, k_{HO^\bullet} and k_{pyr} are the apparent rate constants for the photolytic, degradation by ultrasonically generated oxidative species, molecular/direct with H_2O_2 , radical and thermal decomposition reactions, respectively. C_{TOC} , C_{Ph} , C_{US} , $C_{H_2O_2}$, C_{HO^\bullet} are the concentrations of TOC, photons, oxidative species generated by ultrasonic irradiation, hydrogen peroxide

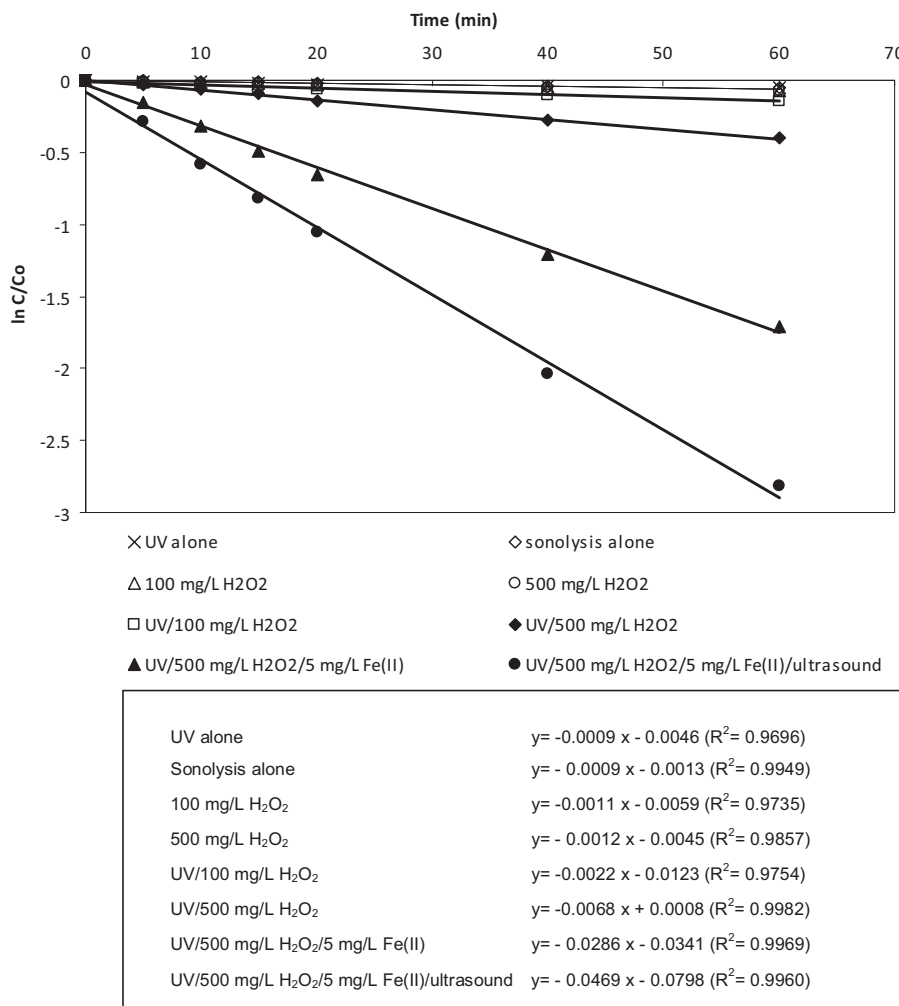


Fig. 6. The pseudo-first order kinetic rate constants in the mineralization reaction of RB4 solutions for different systems. $[TOC]_0 = 30 \text{ mg L}^{-1}$; pH = 3. UV lamp (15 W, 254 nm); amplitude = 60%; pulse length (cycles) = 1. Reaction time = 60 min.

and hydroxyl radicals, respectively. C_{pyr} represents a parameter depending on the temperature inside the bubble, and “ t ” is the reaction time.

It can be assumed for simplicity that the average concentrations of photons, oxidative species generated by ultrasound, H_2O_2 , and HO^\bullet radical and temperature inside the bubble were constant over the reaction time and can therefore be included in the pseudo-first-order kinetics rate constants according to Eq. (23). Thus, the overall mineralization rate (Eq. (22)) can be simplified to a pseudo-first-order kinetic law with respect to the TOC concentration as

follows:

$$\left(-\frac{dC_{\text{TOC}}}{dt} \right)_{\text{overall}} = - (r_{\text{Ph}} + r_{\text{US}} + r_{H_2O_2} + r_{HO^\bullet} + r_{\text{pyr}}) \\ = k'_{\text{Ph}} C_{\text{TOC}} + k'_{\text{US}} C_{\text{TOC}} + k'_{H_2O_2} C_{\text{TOC}} + k'_{HO^\bullet} C_{\text{TOC}} \\ + k'_{\text{pyr}} C_{\text{TOC}} \quad (23)$$

where k'_{Ph} , k'_{US} , $k'_{H_2O_2}$, k'_{HO^\bullet} and k'_{pyr} are the pseudo-first order kinetics rate constants for the photolytic, with ultrasonically

Table 1

Contribution of different reaction mechanisms to overall mineralization of RB4 solutions. $[TOC]_0 = 30 \text{ mg L}^{-1}$; pH = 3; Constants in min^{-1} . UV lamp (15 W).

System	$[KI]$ (mM)	$[H_2O_2]_0$ (mg L^{-1})	$[Fe(II)]_0$ (mg L^{-1})	k_{TOC}	k'_{Ph}	k'_{US}	$k'_{H_2O_2}$	k'_{HO^\bullet}	k'_{pyr}
SPF	No	500	5.0	0.0469	0.0009	0.0009	0.0012	0.0439	0.0000
SPF	2	500	5.0	0.0024	0.0009	0.0003	0.0012	0.0000	0.0000
PF	No	500	5.0	0.0286	0.0009	0.0000	0.0012	0.0265	0.0000
PF	2	500	5.0	0.0021	0.0009	0.0000	0.0012	0.0000	0.0000
SPF	No	500	2.5	0.0130	0.0009	0.0009	0.0012	0.0100	0.0000
SPF	2	500	2.5	0.0024	0.0009	0.0003	0.0012	0.0000	0.0000
SPF	No	500	4.0	0.0188	0.0009	0.0009	0.0012	0.0158	0.0000
SPF	2	500	4.0	0.0024	0.0009	0.0003	0.0012	0.0000	0.0000
SPF	No	500	6.0	0.0329	0.0009	0.0009	0.0012	0.0299	0.0000
SPF	2	500	6.0	0.0024	0.0009	0.0003	0.0012	0.0000	0.0000

SPF: sono-photo-Fenton (amplitude (%): 60; pulse length (cycles): 1).

PF: photo-Fenton (amplitude: NO); pulse length: NO).

generated oxidative species, direct/molecular with H_2O_2 , radical and pyrolytic reactions, respectively:

$$k'_{\text{Ph}} = k_{\text{Ph}} C_{\text{Ph}} \quad (24)$$

$$k'_{\text{US}} = k_{\text{US}} C_{\text{US}} \quad (25)$$

$$k'_{\text{H}_2\text{O}_2} = k_{\text{H}_2\text{O}_2} C_{\text{H}_2\text{O}_2} \quad (26)$$

$$k'_{\text{HO}^\bullet} = k_{\text{HO}^\bullet} C_{\text{HO}^\bullet} \quad (27)$$

$$k'_{\text{pyr}} = k_{\text{pyr}} C_{\text{pyr}} \quad (28)$$

In sono-photo-Fenton reaction, the TOC removal followed pseudo-first-order kinetics with respect to the total organic carbon concentration, as follows:

$$-r = -\frac{dC_{\text{TOC}}}{dt} = k_{\text{TOC}} C_{\text{TOC}} \quad (29)$$

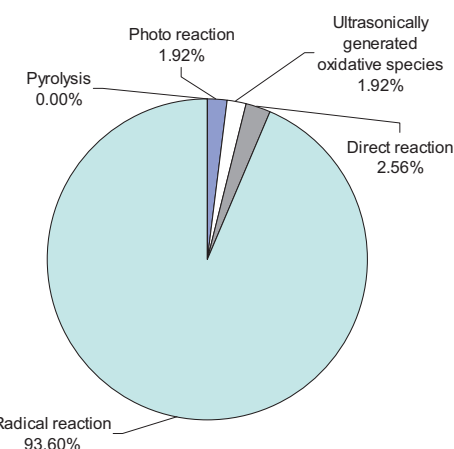
where r is the reaction rate, C_{TOC} is the concentration (mg L^{-1}) of TOC at a given time, t (min) and $k_{\text{TOC}} = (k'_{\text{Ph}} + k'_{\text{US}} + k'_{\text{H}_2\text{O}_2} + k'_{\text{HO}^\bullet} + k'_{\text{pyr}})$ is the pseudo-first-order mineralization rate constant (min^{-1}) for the overall mineralization reaction. This equation can be integrated between $t=0$ and $t=t$, yielding:

$$\ln \frac{C_{\text{TOC}}}{(C_{\text{TOC}})_0} = -k_{\text{TOC}} t \quad (30)$$

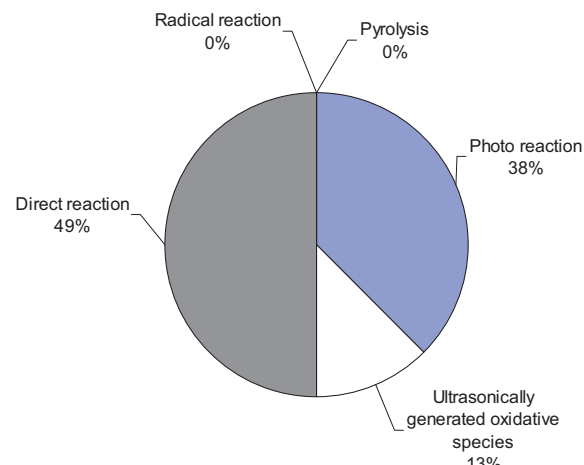
where $(C_{\text{TOC}})_0$ is the initial concentration of TOC. According to this expression, a plot of the first term versus "t" must yield a straight line satisfying Eq. (30) with slope k_{TOC} . (In photo-Fenton reaction, $k_{\text{TOC}} = (k'_{\text{Ph}} + k'_{\text{H}_2\text{O}_2} + k'_{\text{HO}^\bullet})$).

Table 1 shows the values of the constants for the photolytic, with ultrasonically generated oxidative species, direct with H_2O_2 , radical and pyrolytic-thermal reactions corresponding to mineralization process. The photolytic-reaction rate constant, k'_{Ph} , was obtained from the reaction under ultraviolet irradiation alone where free radicals (HO^\bullet) do not occur. The mineralization was due only to light absorption by RB4 molecule and HO^\bullet radicals were not present in solution. k'_{US} was obtained from the reaction by using ultrasonic irradiation alone where a small amount of oxidative species (HO^\bullet , HO_2^\bullet , H^\bullet , H_2O_2) can be generated. The direct/molecular reaction rate constant with hydrogen peroxide, $k'_{\text{H}_2\text{O}_2}$, was calculated from experiments where the only chemical used was H_2O_2 , so in the absence of Fe(II) (HO^\bullet radicals were not present in solution). k_{TOC} was obtained from experiments under the sono-photo-Fenton process. The radical reaction rate constant, k'_{HO^\bullet} , was calculated as follows: $k'_{\text{HO}^\bullet} = [k_{\text{TOC}} - (k'_{\text{Ph}} + k'_{\text{US}} + k'_{\text{H}_2\text{O}_2} + k'_{\text{pyr}})]$. k'_{pyr} was calculated from sono-photo-Fenton reaction in the presence of the radical-scavenging agent potassium iodide (2 mM). HO^\bullet radicals were not present in solution and so the mineralization degree could be mainly attributed to the pyrolytic decomposition inside the bubbles. However, as can be seen in Fig. 7, in the presence of potassium iodide, the mineralization rate is almost negligible as it was only due to the reactions (photolysis + small amounts of oxidative species produced by ultrasonic irradiation (H^\bullet , HO_2^\bullet , H_2O_2)+ direct reaction with H_2O_2 ($k_{\text{TOC}} = k'_{\text{Ph}} + k'_{\text{US}} + k'_{\text{H}_2\text{O}_2}$)). Thus, $k'_{\text{pyr}} = 0$. Similarly, in the photo-Fenton reaction, in the presence of KI, $k_{\text{TOC}} = k'_{\text{Ph}} + k'_{\text{H}_2\text{O}_2}$ (see Table 1). It can be concluded that pyrolytic reaction inside the cavitation bubbles may be excluded since mineralization would occur without interference from KI. Thus, the main mineralization pathway is the radical reaction in the bulk solution or in the vicinity of the bubble, as indicated above.

Fig. 7a shows the importance levels of different mechanisms in the sono-photo-Fenton reaction. Radical reaction is the main mineralization pathway (93.60%). Direct reaction with H_2O_2 represents a 25.6% of reaction. The contribution of photolysis and reaction by



a) Sono-photo-Fenton system in the absence of 2 mM KI. %TOC removal= 94%; $k_{\text{TOC}}= 0.0469 \text{ min}^{-1}$



b) Sono-photo-Fenton system in the presence of 2 mM KI. %TOC removal= 17%; $k_{\text{TOC}}= 0.0024 \text{ min}^{-1}$

Fig. 7. Contributions of photolysis, ultrasonically generated oxidative species, direct oxidation reaction with H_2O_2 , radical reaction (mainly HO^\bullet) and thermal pyrolysis inside the bubble to overall mineralization reaction, in the presence or absence of scavenging agent KI.

ultrasonically generated oxidative species to the overall mineralization is similar, 1.92%. However, as it is shown in Fig. 7b, the contribution of ultrasonically generated oxidative species (13%) is smaller than the photolytic reaction (38%) in the sono-photo-Fenton reaction in the presence of KI (HO^\bullet quencher). In this case, only H^\bullet , HO_2^\bullet and H_2O_2 (ultrasonically generated oxidative species) play a minimal role in mineralization.

Table 1 also shows the importance of the Fe catalyst in the reaction mechanism because of its main role in the sono-photo-Fenton reaction. The radical contribution to overall mineralization increased with Fe(II) (see Fig. 8) since it acts as a catalyst, as indicated above. The radical-mechanism contribution to the mineralization rate increased from 76.92% to 93.60% when Fe concentration increased from 2.5 to 5 mg L^{-1} because more HO^\bullet radicals were available for oxidation. The role of radical reaction decreased to 90.88% when 6 mg L^{-1} Fe(II) was used because an excessive amount of Fe(II) leads to the scavenging of hydroxyl radicals by Fe(II) ions, as indicated above.

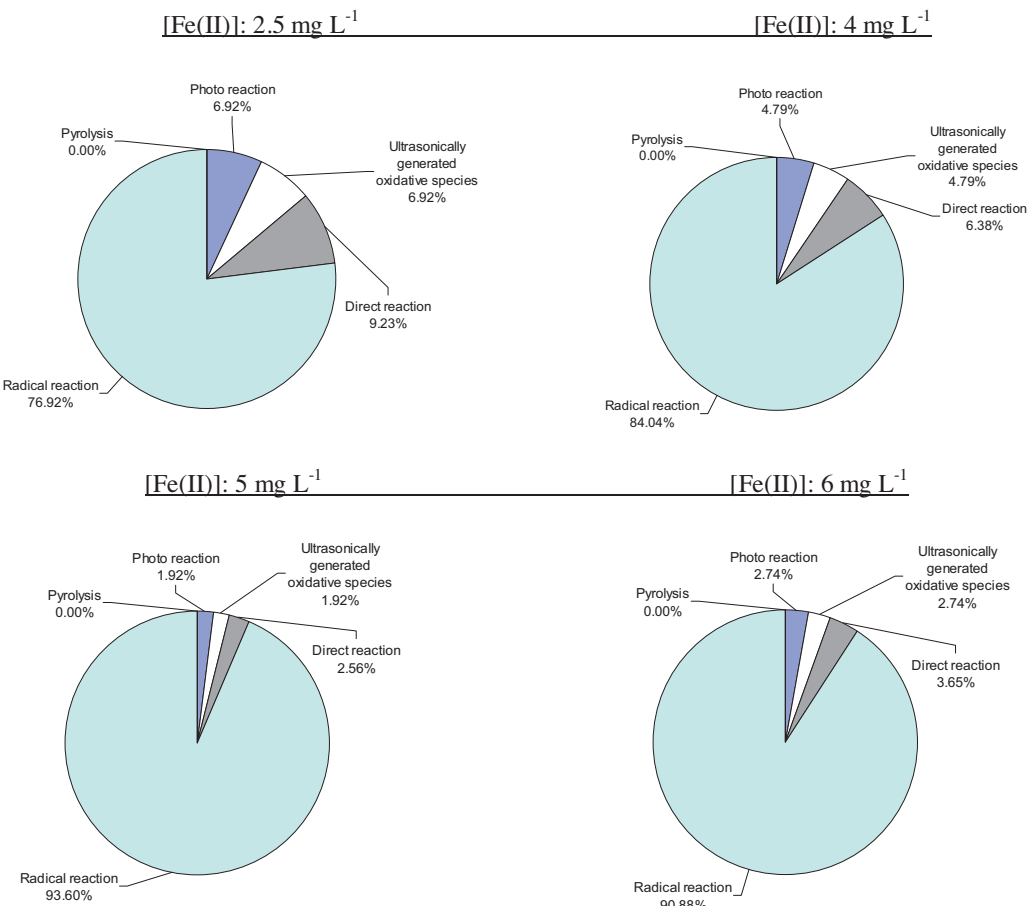


Fig. 8. Role of Fe(II) on radical reaction contribution to overall mineralization reaction. Sono-photo-Fenton process. (a) In the presence of scavenging agent KI; (b) In the absence of scavenging agent KI.

Taking into account the results shown in Fig. 8 and Table 1, when the radical contribution increased, the overall reaction rates also increased as hydroxyl attack is non-selective and faster than the other oxidation pathways.

3.2.6. Toxicity study

No toxicity was detected at the original RB4 solution. Under the conditions employed in this study (sono-photo-Fenton process) no change in toxicity profile was observed after treatment ($EC_{50}(\%) = 193.012$ (no toxic $EC_{50}(\%) > 100$); Equitox = 0.518 (no toxic Equitox < 1)).

4. Conclusions

The use of a homogeneous sono-photo-Fenton process offers a practical alternative for the mineralization of RB4 solutions. Under the optimal conditions ($[Fe(II)]_0 = 5 \text{ mg L}^{-1}$; $[H_2O_2]_0 = 500 \text{ mg L}^{-1}$; $pH = 3$; $[TOC]_0 = 30 \text{ mg L}^{-1}$; UV lamp (15 W, 254 nm); Amplitude = 60%; Pulse length = 1) 94% of TOC is removed after 60 min. An excessive amount of Fe(II) or H_2O_2 leads to a decrease in the degree of mineralization due to the scavenging of hydroxyl radicals. The RB4-mineralization process in the sono-photo-Fenton system can be described by a mechanism involving mineralization by direct photolysis, ultrasonically generated oxidative species, direct oxidation reaction with H_2O_2 , radical reaction (mainly HO^\bullet) and thermal pyrolysis inside the bubble. The ultrasonically generated oxidative species play a minimal role in the mineralization. Pyrolytic reaction inside the bubbles may be excluded since mineralization in the presence of KI is negligible. Fe(II) plays a main role

as a decomposition catalyst in the mineralization reaction of RB4 solution by the sono-photo-Fenton process. No toxic degradation by-products could be detected using *V. fischeri* as test organisms under the conditions employed in the sono-photo-Fenton process.

Acknowledgments

Financial support from the Consejería de Educación y Ciencia of the Junta de Comunidades de Castilla-La Mancha (PCI08-0047-4810 and POII10-0114-3563) is gratefully acknowledged.

References

- [1] J.R. Aspland, *Textile Dyeing and Coloration*, American Association of Textile Chemists and Colorists, Research Triangle Park, NC, 1997.
- [2] F.A.P. Costa, E.M. dos Reis, J.C.R. Azevedo, J. Nozaki, *Solar Energy* 77 (2004) 29–35.
- [3] H. Liu, G. Li, J. Qu, H. Liu, *J. Hazard. Mater.* 144 (2007) 180–186.
- [4] H. Destaillats, A.J. Colussi, J.M. Joseph, M.R. Hoffmann, *J. Phys. Chem. A* 104 (2000) 8930–8935.
- [5] A.S. Ozen, V. Aviyente, G. Tezcanli-Guyer, H. Ince, *J. Phys. Chem. A* 109 (2005) 3506–3516.
- [6] T. Velegraki, I. Poulios, M. Charalabaki, N. Kalogerakis, P. Samaras, D. Mantzavinos, *Appl. Catal. B* 62 (2006) 159–168.
- [7] G. Tezcanli-Guyer, N.H. Ince, *Ultrason. Sonochem.* 10 (2003) 235–240.
- [8] K. Selvam, M. Muruganadham, M. Swaminathan, *Sol. Energy Mater. Sol. Cells* 1 (2005) 1–14.
- [9] I. Arslan-Alaton, G. Tureli, T. Olmez-Hanc, *J. Photochem. Photobiol. A* 202 (2009) 142–153.
- [10] Z. Eren, *J. Environ. Manage.* 104 (2012) 127–141.
- [11] M. Dükkanç, M. Vinatorku, T.J. Mason, *J. Adv. Oxid. Technol.* 15 (2012) 277–283.
- [12] Y.L. Song, J.T. Li, *H. Chem. J. Chem. Technol. Biotechnol.* 84 (2009) 578–583.
- [13] S. Vajnhandl, A.M. Le Marechal, *J. Hazard. Mater.* 141 (2007) 329–335.
- [14] A. Rehorek, M. Tauber, G. Gubitz, *Ultrason. Sonochem.* 11 (2004) 177–182.

- [15] N.A. Jamalluddin, A.Z. Abdullah, *Ultrason. Sonochem.* 18 (2011) 669–678.
- [16] T.J. Mason, J.P. Lorimer, *Sonochemistry*, Ellis Horwood, New York, 1988.
- [17] C. Minero, M. Lucchiari, D. Vione, V. Maurino, *Appl. Catal., B* 39 (2005) 8936–8942.
- [18] Z.H. Ai, L.R. Lu, J.P. Li, L.Z. Zhang, J.R. Qiu, M.H. Wu, *J. Phys. Chem. C* 111 (2007) 4087–4093.
- [19] H. Ghodbane, O. Hamdaoui, *Ultrason. Sonochem.* 16 (2009) 455–461.
- [20] I. Gultekin, G. Tezcanli-Guyer, N.H. Ince, *Ultrason. Sonochem.* 16 (2009) 577–581.
- [21] K.S. Sushlick, *Ultrasound, its chemical*, in: *Physical and Biological Effects*, VCH, Publishers, New York, 1988.
- [22] Y.G. Adewuyi, *Ind. Eng. Chem. Res.* 40 (2001) 4681–4715.
- [23] L.K. Weavers, F.H. Ling, M.R. Hoffmann, *Environ. Sci. Technol.* 32 (1998) 2727–2733.
- [24] R.A. Torres, C. Pétrier, E. Combet, F. Moulet, C. Pulgarín, *Environ. Sci. Technol.* 41 (2007) 297–302.
- [25] H. Katsumata, T. Kobayashi, S. Kaneco, T. Suzuki, K. Ohta, *Chem. Eng. J.* 166 (2011) 468–473.
- [26] M. Dükkanç, M. Vinatoru, T.J. Mason, *Ultrason. Sonochem.* (2013), <http://dx.doi.org/10.1016/j.ultsonch.2013.08.020>.
- [27] P. Vaishnave, A. Kumar, R. Ameta, P.B. Punjabi, S.C. Ameta, *Arabian J. Chem.* (2012), <http://dx.doi.org/10.1016/j.arabjc.2010.12.019>.
- [28] B. Neppolian, H.C. Choi, S. Sakthivel, B. Arabindoo, V. Murugesan, *Chemosphere* 46 (2002) 1173–1181.
- [29] A. Durán, J.M. Monteagudo, M. Mohedano, *Appl. Catal., B* 65 (2006) 127–134.
- [30] P.A. Carneiro, R.F. Pupo Nogueira, M.V.B. Zanoni, *Dyes Pigments* 74 (2007) 127–132.
- [31] A. Durán, J.M. Monteagudo, *Water Res.* 41 (2007) 690–698.
- [32] W.J. Epolito, H. Yang, L.A. Bottomley, S.G. Pavlostathis, *J. Hazard. Mater.* 160 (2008) 594–600.
- [33] J.M. Monteagudo, A. Durán, M. Aguirre, I. San Martin, *J. Hazard. Mater.* 185 (2011) 131–139.
- [34] H.H. Sun, S.P. Sun, J.Y. Sun, R.X. Sun, L.P. Qiao, H.Q. Guo, *Ultrason. Sonochem.* 14 (2007) 761–766.
- [35] R. Chad, N.H. Ince, P.R. Cogate, D.H. Bremer, *Sep. Purif. Technol.* 67 (2009) 103–109.
- [36] J.M. Monteagudo, A. Durán, I. San Martin, A. Carnicer, *Appl. Catal., B* 106 (2011) 242–249.